Journal of Water Process Engineering 21 (2018) 69–76

Contents lists available at ScienceDirect

Journal of Water Process Engineering

journal homepage: www.elsevier.com/locate/jwpe

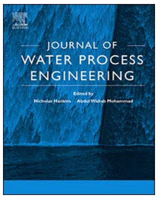

Nano-hematite bagasse composite (*n*-HBC) for the removal of Pb(II) from dilute aqueous solutions

Meina Liang[a,b], Dunqiu Wang[a,b,*], Yinian Zhu[a,b], Zongqiang Zhu[b,c], Yanhong Li[b], C.P. Huang[c,**]

[a] *College of Light Industry and Food Engineering, Guangxi University, Nanning 530004, PR China*
[b] *College of Environmental Science and Engineering, Guilin University of Technology, Guilin 541004, PR China*
[c] *Department of Civil and Engineering, University of Delaware, Newark, DE 19716, United States*

ARTICLE INFO

Keywords:
Nano-hematite bagasse composite (*n*-HBC)
Lead(II)
Surface complex formation
Adsorption
Impregnation

ABSTRACT

Nano-hematite bagasse composite (*n*-HBC) was synthesized, characterized and tested for the removal of Pb(II) from dilute aqueous solutions. The particle size of ferric oxide was in the range of 100–300 nm. The composite surface, both internal and external, was occupied by abundant oxygen-containing functional groups. The optimum Pb(II) adsorption density occurred in the pH range from 4.0 to 5.5. Adsorption reached equilibrium rapidly in 480, 600, 720 min at initial Pb(II) concentration of 20, 30, and 40 mg/L, respectively, at 25 °C and pH 5.0. The maximum Pb(II) adsorption capacity, calculated from the Langmuir adsorption isotherm, was 16.57 mg/g at 25 °C. Furthermore, surface complexation model was also applied to describe the adsorption reaction between aqueous Pb(II) and *n*-HBC. The Gibbs free energy of adsorption, ΔG_{ads}^{0}, was −39.49 kJ/mol (9.44 kcal/mol) at 25 °C, which indicated spontaneous Pb(II) ion adsorption on *n*-HBC. Results of XPS studies demonstrated the presence of surface oxygen-containing functional groups, which were involved in the adsorption of Pb(II) and that hematite played a key role in Pb (II) uptake.

1. Introduction

Lead(II) is known toxic chemical species in water. High lead(II) concentration in drinking water is known to have adverse human health effects, such as anemia, kidney failure, mental retardation, and physiological defects [1]. Lead(II) in the aquatic environment may originate from mainly from anthropogenic activities. Many methods such as coagulation, chemical precipitation, solvent extraction, membrane separation, reverse osmosis, ion exchange, and adsorption have been used to remove heavy metals, including lead(II), from water and wastewater [2–4]. Among all of these methods, adsorption is a simple, effective, and inexpensive process for Pb(II) removal from dilute aqueous solutions [5]. Activated carbon, due to its large specific surface area, microporous structure, and stable chemical properties, has been widely used for environmental remediation practices including water purificaiton. Wood and coal are generally the major raw materials for activated carbon manufacturing. However, the availability of these raw materials has prompted several studies to use waste agricultural by-products for the removal of metals from water and wastewater [6–8]. Activated carbon has been reported effective in removing Pb(II) from wastewater [9–11]. Huang et al. [12–19,58] were among the early researchers to study the adsorption of heavy metals from water by commercial activated carbon. Imamoglu and Tekir [20] studied the removal of Cu(II) and Pb(II) from water using activated carbon prepared from hazelnut husks. Song et al. [21] reported effective removal of Pb(II) using a surface modified coconut-based activated carbon. While results of the above studies generally showed effective removal of lead from wastewater at high concentrations, Pb(II) removal at dilute concentration was rather inefficient. Therefore, absorbents with strong adsorption capability over an extended concentration range for metal removal from water are needed.

Iron oxide, with pH_{zpc} in the neutral pH range and capable of removing a wide group of cations and anions, has received considerable attention [22–24]. Raven et al. reported high adsorption capacity toward Pb(II), Cu(II), Zn(II), Ni(II), and Cr(VI) by iron-based adsorbents [25,26]. However, iron-based adsorbents had relatively small specific surface area, slow mass transfer, and low recycle/reuse potential [27]. Therefore; there are interests in activated carbon-iron oxide composites. Bagasse is a solid residue from the sugar cane refinery industry and can be a sustainable resource of material for the preparation of activated carbon [28].

In this study, we prepare a nano-hemite-bagasse composite (*n*-HBC)

---

[*] Corresponding author at: College of Light Industry and Food Engineering, Guangxi University, Nanning 530004, PR China.
[**] Corresponding author at: Department of Civil and Environmental Engineering, University of Delaware, Newark, DE 19716, United States.
E-mail addresses: wangdunqiu@sohu.com (D. Wang), huang@udel.edu (C.P. Huang).

https://doi.org/10.1016/j.jwpe.2017.11.014
Received 5 September 2017; Received in revised form 17 November 2017; Accepted 26 November 2017

and study the Pb(II) adsorption characteristics of this material. Factors such as contact time, pH, Pb(II) concentration, and bagasse content on the metal adsorption capacity of *n*-HBC were studied first in batch experiments. Pb(II) adsorptipon characteristics on hydrous *n*-HBC described in terms of Langmuir adsorption isotherm and surface complex formation model.

2. Materials and methods

2.1. Materials

All chemicals/reagents used in the study were of analytical grade and used without further purification except lead standard solution. Ferric chloride hexahydrate ($FeCl_3{\cdot}6H_2O$), ammina ($NH_3{\cdot}H_2O$), sodium hydroxide (NaOH), nitric acid (HNO_3), lead nitrate ($Pb(NO_3)_2$), sodium chloride (NaCl) and cetyl-trimethyl ammonium bromide (CTMAB) were purchased from Country Medicine Group in Shanghai, China. Bagasse was obtained from a sugar industry site in Guangxi, China.

2.2. Preparation of n-HBC

First, bagasse was dried in an oven at 80 °C for 24 h then ground into small size and sieved to an average particle size of 5 mm. One mol/L of $FeCl_3$, 0.05 mol/L of (CTMAB) and 10% (v/v) of ammonia solution, all of analytical grade, were prepared with ultrapure water. Add CTMAB, (100 mL at 0.05 mol/L) and ultrapure water (800 mL) into a 2-L beaker and heated to boiling. Then, added 100 mL of 1 mol/L $FeCl_3$ solution to the boiling solution while slowly stirring to obtain a red-brown colloid solution. Mixed fifty gram dried bagasse with the colloid solution. After mixing for 24 h, the pH value of the mixture was adjusted to 7.4 with 10% (v/v) ammonia solution using an automatic potentiometric titrator (Metrohm 848 Titrino Plus) to produce bagasse–ferric hydroxide composite. The solid was filtered and dried in an oven at 105–110 °C for 24 h followed by drying in a muffle furnace to collect nano-$Fe(OH)_3$-bagsse solid, which was then carbonized/activated at 550 °C for 4 h to obtain *n*-HBC [29]. For the purpose of comparison, carbonized bamboo biochar without nnao-hematite was prepared. Briefly, the dried bamboo biochar (average particle size 5 mm) was heated at 550 °C for 4 h in a muffle furnace at a heating rate of 4 °C per min then allowed to cool to room temperature.

2.3. Batch adsorption experiments

Batch Pb(II) removal experiments were conducted first. A desired amount of *n*-HBC powder was weighted and put in a series of plastic centrifuge tubes (100 mL) and added 50 mL solution of different Pb(II) concentrations (i.e., 20–50 mg/L). After adjusting the pH, with NaOH (0.1 M) or HNO_3 (0.1 M), to pre-selected value the centrifuge tubes were sealed with capsules and placed on a temperature shaker (i.e., 25°, 35° or 45 °C) and shaken at a speed of 200 strokes per min to attain adsorption equilibrium. After centrifugation at 4000 rpm for 5 min, the supernatant was filtered through 0.45-μm micro-pore membrane and added 0.2% (V/V) HNO_3 to stabilize the sample in 100 mL volumetric flask before analyzing for the residual Pb(II). Samples were stored in acid-washed high-density polyethylene containers until analysis of residual Pb(II). All samples were analyzed within three days of collection.

The adsorption capacity of *n*-HBC at time, *t*, was calculated according to the mass balance relationship of Pb(II) ions expressed as:

$$q = \left(\frac{V}{X}\right) \times (C_o - C_t) \tag{1}$$

where C_0 and C_t are Pb(II) concentration (in mg/L) at initial and time *t*, respectively. *V* is the volume of the solution (L) and X is the mass of the *n*-HBC used (g). The percent Pb(II) removal, R, was determined by the following equation:

$$R(\%) = 100 \times \left(\frac{C_o - C_t}{C_o}\right) \tag{2}$$

2.4. Experimental conditions

The effect of various operating parameters, namely, contact time (30–1200 min), solution pH (2.0–9.0), adsorbent dosage (0.67-2.67 g/L), initial Pb(II) concentration (20–50 mg/L) and temperature (298–318 K), on Pb(II) adsorption were studied first. The adsorption isotherm, adsorption rate, and thermodynamic parameters at pH 5.0 were obtained and analyzed as well.

2.5. Surface characterization of n-HBC

Specific surface area was determined according to the Brunauer–Emmet–Teller (BET) equation by nitrogen gas adsorption using a Quantachrome Nova Station apparatus. Surface charge was determined by alkalimetric titration of 0.2 g/L solid suspension with NaOH (10^{-3} M) and HCl (10^{-3} M) in NaCl(10^{-2} M) as supporting electrolyte. The pH value was recorded using a pH meter, model PB-10 (Sartorius Co. Germany). Additionally, the zeta potential of the adsorbent was measured as a function of pH in NaCl(10^{-2} M) electrolyte using Nanoparticle & Zeta Potential Analyzer, model ZS90 (Malvern Co. England).

The structural feature of the *n*-HBC was observed using Hitachi S-4800 scanning electron microscope (SEM) at the acceleration voltage of 10 kV. Infrared spectra (FTIR) were obtained using KBr pellets (Acros, IR grade 99%, 1 mg of solid with 150 mg of KBr) with a Thermo Nicolet Nexus 470 Fourier transform spectrometer at 2 cm^{-1} resolution. X-ray diffraction (XRD) analysis on a X'Pert PRO X diffractometer using filtered copper Kα radiations. XPS experiments were performed with ESCALAB 250Xi using an Al Kα X-ray source (1486.6 eV). A nonlinear least-square curve-fitting program (XPSPEAK software 4.1, Raymund W. M. Kwork) was used to deconvolve the XPS data. Residual Pb(II) concentration was determined by atomic absorption spectrometer (Perkin Elmer AAnalyst 700).

3. Results and discussions

3.1. Surface characteristics of n-HBC

Fig. 1a shows the SEM images of *n*-HBC. The size and shape of nano-hematite particles on *n*-HBC could be seen from the SEM images. The size and shape of nano-hematite particles on *n*-HBC could be seen from the SEM images. The size of nano-hematite particles was in the range of 50 and 100 nm. Fig. 1b shows XRD spectra of *n*-HBC. All major peaks could be clearly seen and identified as standard hematite (α-Fe_2O_3) (00-033-0664), confirming the formation of hematite (α-Fe_2O_3) during preparation. Fig. 1c shows the FTIR spectra of *n*-HBC. The absorption peaks were at 3426, 2924, 2852, 1630, 1400, 1170, 1120 and 610 cm^{-1}, respectively. The =C=O functional groups were at 1630 cm^{-1} and −OH functional groups appeared at 3426 cm^{-1}. The peak at 2852 cm^{-1} was attributed to C−H stretching vibration. The peak at 1400 cm^{-1} was associated with −OH bending deformation in carbocyclic acids and phenolic groups. The adsorption band at 1170 cm^{-1} was asymmetric stretching of the C−O−C bridge. The peak at 1120 cm^{-1} was attributed to some overtones. The oxygen-containing functional groups were present abundantly on the external and internal surfaces of *n*-HBC, as adsorption sites and contributed to the adsorption capacity of *n*-HBC. The FTIR spectra of *n*-HBC were different from that of oxidized activated carbon reported by Ding et al. [30]. Ding et al. [30] reported that the peaks at 2338 cm^{-1} due to C≡C stretching and 1722 and 1595 cm^{-1} due to C=O stretching were reduced, and the peaks at 1061 cm^{-1} due to C−O stretching disappeared upon heating at 550 °C. They also suggested that heating at elevating temperature